*Acta Oceanol. Sin.*, 2021, Vol. 40, No. 1, P. 54–61
https://doi.org/10.1007/s13131-020-1699-5
http://www.hyxb.org.cn
E-mail: hyxbe@263.net

# Theoretical analysis of equatorial near-inertial solitary waves under complete Coriolis parameters

Ruigang Zhang[1], Liangui Yang[1]*
[1] School of Mathematical Sciences, Inner Mongolia University, Hohhot 010021, China

Received 6 November 2019; accepted 9 December 2019



**Abstract**

An investigation of equatorial near-inertial wave dynamics under complete Coriolis parameters is performed in this paper. Starting from the basic model equations of oceanic motions, a Korteweg de Vries equation is derived to simulate the evolution of equatorial nonlinear near-inertial waves by using methods of scaling analysis and perturbation expansions under the equatorial beta plane approximation. Theoretical dynamic analysis is finished based on the obtained Korteweg de Vries equation, and the results show that the horizontal component of Coriolis parameters is of great importance to the propagation of equatorial nonlinear near-inertial solitary waves by modifying its dispersion relation and by interacting with the basic background flow.

**Key words:** complete Coriolis parameters, equatorial nonlinear near-inertial waves, Korteweg de Vries equation, solitary waves

**Citation:** Zhang Ruigang, Yang Liangui. 2021. Theoretical analysis of equatorial near-inertial solitary waves under complete Coriolis parameters. Acta Oceanologica Sinica, 40(1): 54–61, doi: 10.1007/s13131-020-1699-5

## 1 Introduction

The influence of the atmosphere and ocean on human beings has always been a topic of interest for scientists (Nezlin and Snezhkin, 1993) because it is useful to understand the physical mechanisms of atmospheric or oceanic motions to further predict extreme weather or climate phenomena. Theoretically, a series of primitive partial differential equations, including the mass, momentum, state and so on, are used to characterize the motions of the atmosphere and ocean (Pedlosky, 1987). The motions of the atmosphere and ocean are affected by multiple physical factors, such as gravitation, Coriolis force, and friction. This leads to multiscale motions from turbulent microclusters and planetary waves for geophysical fluids. Existing theories have shown that it is appropriate to classify the motions of geophysics into three categories, i.e., large-scale, mesoscale and small-scale motions (Holton and Hakim, 2013). Large-scale motions, such as planetary waves, show that the rotation of the earth is extremely important; it is mainly used to disclose the physical mechanisms of the slowly varying phenomena for the atmosphere or ocean, and more details can be found in other studies (Long, 1964; Benney, 1966; Ono, 1981; Caillol and Grimshaw, 2008; Guo et al., 2019; Fu et al., 2019; Fu and Yang, 2019; Ren et al., 2019; Zhang et al., 2019a, 2019b; Zhang and Yang, 2019). Mesoscale atmospheric and oceanic motions characterize wave phenomena, such as the internal waves, under the combined actions of gravity, pressure, Coriolis force (Khater et al., 2006b; Helal and Seadawy, 2012; Seadawy, 2017a, 2018; Seadawy and Alamri, 2018; Yang et al., 2019). Mesoscale motions have received increased attention from investigators because they can help us understand the excitation, evolution, and propagation of a class of weather events, such as thunderstorms and rainstorms. Small-scale oceanic motions generally describe the fluctuations with vertical length scale from 100 m to the atomic dissipation, including the fine-structure process and micro-structure process (Caldwell, 1983).

Simplified and approximate models have always been important ways to understand various wave phenomena in the atmosphere and ocean because of the complexity of the original primitive model equations. For example, the Boussinesq approximation and shallow water approximation are usually used to model large-scale motions (Pedlosky, 1987). The shallow water approximation neglects the terms related to the horizontal component of Coriolis parameters in the momentum equations, which is often called the “traditional approximation” (Phillips, 1966). The “traditional approximation” is suitable for large-scale longwave theory, which ensures the conservation of angular momentum, vorticity and energy concerning horizontal movements without considering vertical directional motions. However, with the development of higher precision science and technology and with the requirements for more accurate weather predictions, it has been suggested that the full Coriolis force should be considered, which is called “nontraditional approximation” (White and Bromley, 1995). When the complete Coriolis parameters are considered (Gerkema et al., 2008; Leibovich and Lele, 1985), the results show that the deviation is small compared to the geostrophic wind for large-scale quasi-geostrophic motion, but it reflects the imbalance of motion, and the inclusion of complete Coriolis parameters is an important factor causing the development of weather systems. In particular, the “nontraditional ap-

Foundation item: The National Natural Science Foundation of China under contract No. 11762011; the Natural Science Foundation of Inner Mongolia Autonomous Region under contract No. 2020BS01002; the Research Program of Science at Universities of Inner Mongolia Autonomous Region under contract No. NJZY20003; the Scientific Starting Foundation of Inner Mongolia University under contract No. 21100-5185105.
*Corresponding author, E-mail: lgyang@imu.edu.cn

proximation" is more important for near-equatorial atmosphere and ocean than that in mid-latitude, and it is noted as potential contributing to equatorial Madden-Julian Oscillation (MJO) phenomena and oceanic circulation phenomena (Hayashi and Itoh, 2012).

More importantly, the vertical velocities of mesoscale systems are larger than those of large-scale motions by one or several orders. Thus, the divergence and vorticity of mesoscale motions have larger magnitudes than those of large-scale motions. The effects of the horizontal component of Coriolis parameters on mesoscale atmospheric or oceanic motions, such as the Ekman spiral (Marshall and Schott, 1999), near-inertial waves (Zhang, 1991), deep convection (Kasahara, 2010), and internal waves (Satsuma et al., 1979; Liu et al., 2015), have received increased attention. Grimshaw (1975) studied the effect of the horizontal component of Coriolis parameters on internal gravity waves in the early stage. Fruman (2009) discussed various wave forms under the action of complete Coriolis force, such as the Kelvin wave, Rossby wave, inertial gravity wave and mixed wave. In particular, when the internal or near-inertial waves in the ocean have weak stratification, the effect of "nontraditional approximation" is more obvious compared to the case under traditional approximation. The results showed that the complete Coriolis force in the mesoscale range of motion represents a nonstatic effect, which has an important impact on the dispersion and instability of near-inertial waves (Gerkema and Shrira, 2005a, b). Yasuda and Sato (2013) discussed the effect of the horizontal component of Coriolis parameters on linear near-inertial waves. Kasahara (2003) considered the nonstatic model of mid-latitude under beta-plane approximation and illustrated the importance of the complete Coriolis force in inducing linear inertial waves (BII waves) at the boundary. White and Bromley (1995) pointed out that cumulus convection could be accompanied by adiabatic heating as hot air rises in the equatorial region through scale analysis. They noted that the horizontal component of the Coriolis parameter in the latitudinal momentum equation cannot be ignored, which is one of the reasons for the generation of near-inertial waves at the equator. Furthermore, the "nontraditional approximation" would increase inertial instability (Itano and Kasahara, 2011). Kloosterziel et al. (2007) studied the zonal symmetric inertial instability of ocean motion in the near-equatorial region through high-resolution numerical simulation. Recently, Yano (2017) considered the inertial gravity wave under the action of the complete Coriolis force. It was said that the complete Coriolis force is essentially important for the high-order problem of the degenerated system under the limit of the horizontal wavelet number. In conclusion, buoyancy and rotation are two basic factors determining mesoscale circulation, so the influences of density stratification and the horizontal component of the Coriolis parameter on mesoscale waves are quite important, especially for near-inertial waves. Thus, there are many difficulties in the study of related problems because of the density stratification of fluids and the introduction of the complete Coriolis force.

However, most existing studies neglect the nonlinear effect and vertical acceleration, which is the essence of the nonlinear wave. This paper intends to conduct a thorough study on nonlinear near-inertial waves under complete Coriolis parameters using mathematical mechanics, providing an important theoretical basis for the research and application of numerical weather forecasting and weather event phenomena in the atmosphere and ocean. The paper is organized as follows. In Section 2, a mathematical description of the atmospheric or oceanic motions is given. In Section 3, the simplified model is derived according to the scale analysis. In Section 4, a Korteweg de Vries (KdV) model equation is obtained to simulate the evolution of equatorial near-inertial waves by using the multiple scale method and perturbation expansions. The exact solutions, including the periodic and solitary solutions, for the obtained KdV equation are given. In Section 5, the dynamic effect of the horizontal component of Coriolis parameters on the equatorial near-inertial waves is assessed by numerical simulation. Conclusions are offered at the end of the paper.

## 2 Mathematical model

In this article, we consider the mesoscale oceanic model under the complete Coriolis parameters, but without the effects of topography, dissipation, adiabatic heating or any other factors. It is written as follows in the local Cartesian coordinate system:

$$\begin{cases} \dfrac{\partial u}{\partial t}+u\dfrac{\partial u}{\partial x}+v\dfrac{\partial u}{\partial y}+w\dfrac{\partial u}{\partial z}=-\dfrac{1}{\rho_0}\dfrac{\partial p}{\partial x}+fv-f'w, \\ \dfrac{\partial v}{\partial t}+u\dfrac{\partial v}{\partial x}+v\dfrac{\partial v}{\partial y}+w\dfrac{\partial v}{\partial z}=-\dfrac{1}{\rho_0}\dfrac{\partial p}{\partial y}-fu, \\ \dfrac{\partial w}{\partial t}+u\dfrac{\partial w}{\partial x}+v\dfrac{\partial w}{\partial y}+w\dfrac{\partial w}{\partial z}=-\dfrac{1}{\rho_0}\dfrac{\partial p}{\partial z}+g\dfrac{\theta}{\theta_0}+f'u\ , \\ \dfrac{\partial \theta}{\partial t}+u\dfrac{\partial \theta}{\partial x}+v\dfrac{\partial \theta}{\partial y}+\sigma w=0, \\ \dfrac{\partial(\rho_0 u)}{\partial x}+\dfrac{\partial(\rho_0 v)}{\partial y}+\dfrac{\partial(\rho_0 w)}{\partial z}=0, \end{cases} \tag{1}$$

where $x$, $y$ and $z$ are the zonal, meridional and vertical coordinates, and $u$, $v$, $w$ are the velocities, accordingly. $\rho_0, \theta_0$ are the density and potential temperature in the ambient flow field, respectively, they are expressed as functions of $z$, and the temperature stratification is defined as $\sigma=\dfrac{\mathrm{d}\theta_0}{\mathrm{d}z}$. $\theta$ is the perturbation of temperature. The vertical component of the equatorial Coriolis parameters is $f=f_0+\beta y$ with $f_0=0$, thus,

$$f=\beta y. \tag{2}$$

The beta parameter in the equatorial region is $\beta=2\Omega/a_0$, where $\Omega$ is the angular velocity of the earth's rotation and $a_0$ is the radius of the earth. At the same time, the horizontal component of the Coriolis parameters is $f'=2\Omega$, and it is constant. $p$ is the pressure, and $g$ is the gravitational acceleration.

## 3 Scale analysis

We introduce the nondimensional quantities as follows:

$$\begin{cases} (u,v)=U(u',v'), \\ w=\dfrac{U}{L}D(w'), \\ \rho_0=\dfrac{P}{gH}(\rho_s), \\ (x,y)=L(x',y'), \\ z=D(z'), \\ t=(\beta L)^{-1}(t'), \\ \theta=\delta\theta(\theta'), \\ \delta p_{x,y}=\dfrac{\beta PL^2U}{gH}(p'), \\ \delta p_z=\dfrac{P}{\theta_0}\delta\theta(p'), \end{cases} \tag{3}$$

where $L$ and $U$ are the horizontal characteristic length and characteristic velocity, $D$ is the vertical characteristic length, $H$ is the homogeneous atmospheric height, and it is assumed that $D=H$. $P$ is the characteristic pressure, and the changes of pressures in the horizontal and vertical directions are presented by $\delta p_{x,y}$ and $\delta p_z$. $\rho_s$ is the nondimensional density, and $g$ is the gravitational acceleration. The quantities with apostrophes represent dimensionless ones. The nondimensional equations are obtained by substitutions of Eqs (2) and (3) into Eq. (1)

$$\begin{cases} \dfrac{\partial u'}{\partial t'} + Ro\left(u'\dfrac{\partial u'}{\partial x'} + v'\dfrac{\partial u'}{\partial y'} + w'\dfrac{\partial u'}{\partial z'}\right) = -\dfrac{1}{\rho_s}\dfrac{\partial p'}{\partial x'} + \\ yv' - \alpha w', \\ \dfrac{\partial v'}{\partial t'} + Ro\left(u'\dfrac{\partial v'}{\partial x'} + v'\dfrac{\partial v'}{\partial y'} + w'\dfrac{\partial v'}{\partial z'}\right) = -\dfrac{1}{\rho_s}\dfrac{\partial p'}{\partial y'} - yu', \\ \dfrac{\partial w'}{\partial t'} + Ro\left(u'\dfrac{\partial w'}{\partial x'} + v'\dfrac{\partial w'}{\partial y'} + w'\dfrac{\partial w'}{\partial z'}\right) = \dfrac{g\delta\theta}{\beta UD\theta_0}\times \\ \left(-\dfrac{1}{\rho_s}\dfrac{\partial p'}{\partial z'} + \theta'\right) + \lambda u', \\ \dfrac{\partial \theta'}{\partial t'} + Ro\left(u'\dfrac{\partial \theta'}{\partial x'} + v'\dfrac{\partial \theta'}{\partial y'}\right) + \dfrac{\sigma UD}{\beta L^2\delta\theta}w' = 0, \\ \dfrac{\partial(\rho_s u')}{\partial x'} + \dfrac{\partial(\rho_s v')}{\partial y'} + \dfrac{\partial(\rho_s w')}{\partial z'} = 0, \end{cases} \tag{4}$$

where $Ro=\dfrac{U}{\beta L^2}$ is the equatorial Rossby number, and $\gamma=\dfrac{f'}{\beta L}$ represents the ratio of the horizontal component to the vertical component of the equatorial Coriolis parameters; $\delta=\dfrac{D}{L}$ is expressed as the aspect ratio of the motion. $\alpha=\gamma\delta$ and $\lambda=\dfrac{\gamma}{\delta}$ represent the combined influences of the horizontal component of Coriolis parameters and the aspect ratio on the equatorial near-inertia fluctuations. This shows that the three-dimensional fluctuation is a necessary condition for studying the complete Coriolis force, which means that it is not sufficient to add the horizontal component of the Coriolis parameters into the shallow water model in the traditional sense. Furthermore, the quantitative comparison between $\lambda$ and $\alpha$ reveals a relatively greater influence of $\lambda$ than $\alpha$ on the motion.

In fact, the condition $U=C_g$ is almost satisfied for the equatorial atmospheres, where $C_g$ is the characteristic velocity of the gravity wave. The time scale is

$$T = (\beta L)^{-1} = \frac{L}{U}, \tag{5}$$

and then $T=\dfrac{L}{C_g}=(\beta C_g)^{-\frac{1}{2}}$. In the lower tropical area, the following assumptions are satisfied with $C_g\approx 10^2$ m/s, $\beta\approx 2.3\times 10^{-11}$ $(\text{m}\cdot\text{s})^{-1}$, $L\approx 2\times 10^6$ m, $T\approx 6$ h, $U\approx 20$ m/s. Thus, it is acceptable that $Ro\approx 1$ in the tropics, and ignoring $Ro$ is not appropriate for our further study. We take $Ro\approx 1$ in the tropics, and ignoring $Ro$ is not appropriate for our further study. We take $Ro\approx 1$ in what follows according to the above discussions. The second term of the fourth equation in Eq. (4) is generally small by the scale balance principle; it is known that

$$\delta\theta = \frac{\sigma UD}{\beta L^2}, \tag{6}$$

thus $\dfrac{g\delta\theta}{\beta UD\theta_0}=\dfrac{N^2}{\beta C_g}$, where $N^2=g\sigma/\theta_0$ is the Brunt-Väisälä frequency. Denote

$$\frac{\beta C_g}{N^2} = \varepsilon, \tag{7}$$

then $\varepsilon << 1$. When the dimensionless apostrophes are omitted, Eq. (4) becomes

$$\begin{cases} \dfrac{\partial u}{\partial t} + u\dfrac{\partial u}{\partial x} + v\dfrac{\partial u}{\partial y} + w\dfrac{\partial u}{\partial z} = -\dfrac{1}{\rho_s}\dfrac{\partial p}{\partial x} + yv - \alpha w, \\ \dfrac{\partial v}{\partial t} + u\dfrac{\partial v}{\partial x} + v\dfrac{\partial v}{\partial y} + w\dfrac{\partial v}{\partial z} = -\dfrac{1}{\rho_s}\dfrac{\partial p}{\partial y} - yu, \\ \dfrac{\partial w}{\partial t} + u\dfrac{\partial w}{\partial x} + v\dfrac{\partial w}{\partial y} + w\dfrac{\partial w}{\partial z} = \varepsilon^{-1}\left(-\dfrac{1}{\rho_s}\dfrac{\partial p}{\partial z} + \theta\right) + \lambda u, \\ \dfrac{\partial \theta}{\partial t} + u\dfrac{\partial \theta}{\partial x} + v\dfrac{\partial \theta}{\partial y} + w = 0, \\ \dfrac{\partial(\rho_s u)}{\partial x} + \dfrac{\partial(\rho_s v)}{\partial y} + \dfrac{\partial(\rho_s w)}{\partial z} = 0. \end{cases} \tag{8}$$

## 4 Derivation of the evolution equation

### 4.1 *Multiple scales and perturbation method*

Many kinds of PDEs have been derived to simulate the evolution of waves (Khater et al., 2006a; Seadawy, 2011; 2015; 2016; 2017b; Seadawy et al., 2017; Tian et al., 2019). Here, we use the KdV model equation. To balance the dispersion and nonlinearity, we introduce

$$\begin{cases} \dfrac{\partial}{\partial t} = \varepsilon^{\frac{1}{2}}\left(-c\dfrac{\partial}{\partial \xi} + \varepsilon\dfrac{\partial}{\partial T}\right), \\ \dfrac{\partial}{\partial x} = \varepsilon^{\frac{1}{2}}\dfrac{\partial}{\partial \xi}, \\ \dfrac{\partial}{\partial y} = \dfrac{\partial}{\partial y}, \\ \dfrac{\partial}{\partial z} = \dfrac{\partial}{\partial z}, \end{cases} \tag{9}$$

where $T$, $\xi$ are slowly varying. $u$, $v$, $w$, $p$, $\theta$ are expanded:

$$\begin{cases} u = \bar{u}(y,z) + \varepsilon(u_0 + \varepsilon u_1 + \varepsilon^2 u_2 + \cdots), \\ v = \varepsilon^{\frac{3}{2}}(v_0 + \varepsilon v_1 + \varepsilon^2 v_2 + \cdots), \\ w = \varepsilon^{\frac{3}{2}}(w_0 + \varepsilon w_1 + \varepsilon^2 w_2 + \cdots), \\ \theta = \bar{\theta}(y,z) + \varepsilon(\theta_0 + \varepsilon\theta_1 + \varepsilon^2\theta_2 + \cdots), \\ p = \bar{p}(y,z) + \varepsilon(p_0 + \varepsilon p_1 + \varepsilon^2 p_2 + \cdots). \end{cases} \tag{10}$$

Substitutions of Eqs (9) and (10) into Eq. (8) yield an order equation. The lowest-order problem is

$$\begin{cases} -\dfrac{1}{\rho_s}\dfrac{\partial \bar{p}}{\partial y} - y\bar{u} = 0, \\ -\dfrac{1}{\rho_s}\dfrac{\partial \bar{p}}{\partial z} + \bar{\theta} = 0. \end{cases} \tag{11}$$

Equation (11) indicates that the basic flow satisfies the equatorial semigeostrophic equilibrium and static equilibrium. When $\left|\dfrac{1}{\rho_s^2}\dfrac{\partial \rho_s}{\partial z}\right| << 1$, the thermal wind is

$$\frac{\partial \bar{\theta}}{\partial y} = -y\frac{\partial \bar{u}}{\partial z}. \tag{12}$$

Thus, the lowest order equation reveals information of the background flow, but without any information about the perturbation flow. We further consider the higher orders with representations of

$$\begin{cases}(\bar{u}-c)\dfrac{\partial u_0}{\partial \xi}+(\bar{u}_y-y)v_0+(\bar{u}_z+\alpha)w_0+\dfrac{1}{\rho_s}\dfrac{\partial p_0}{\partial \xi}=0,\\ \dfrac{1}{\rho_s}\dfrac{\partial p_0}{\partial y}+yu_0=0,\\ -\dfrac{1}{\rho_s}\dfrac{\partial p_0}{\partial z}+\theta_0+\lambda\bar{u}=0,\\ (\bar{u}-c)\dfrac{\partial \theta_0}{\partial \xi}+\bar{\theta}_y v_0+w_0=0,\\ \dfrac{\partial(\rho_s u_0)}{\partial \xi}+\dfrac{\partial(\rho_s v_0)}{\partial y}+\dfrac{\partial(\rho_s w_0)}{\partial z}=0,\end{cases} \tag{13}$$

and

$$\begin{cases}(\bar{u}-c)\dfrac{\partial u_1}{\partial \xi}+(\bar{u}_y-y)v_1+(\bar{u}_z+\alpha)w_1+\dfrac{1}{\rho_s}\dfrac{\partial p_1}{\partial \xi}=\\ \quad -\left(\dfrac{\partial u_0}{\partial T}+u_0\dfrac{\partial u_0}{\partial \xi}+v_0\dfrac{\partial u_0}{\partial y}+w_0\dfrac{\partial u_0}{\partial z}\right),\\ \dfrac{1}{\rho_s}\dfrac{\partial p_1}{\partial y}+yu_1=-(\bar{u}-c)\dfrac{\partial v_0}{\partial \xi},\\ \dfrac{1}{\rho_s}\dfrac{\partial p_1}{\partial z}-\theta_1=\lambda u_0,\\ (\bar{u}-c)\dfrac{\partial \theta_1}{\partial \xi}+\bar{\theta}_y v_1+w_1=-\left(\dfrac{\partial \theta_0}{\partial T}+u_0\dfrac{\partial \theta_0}{\partial \xi}+v_0\dfrac{\partial \theta_0}{\partial y}\right),\\ \dfrac{\partial(\rho_s u_1)}{\partial \xi}+\dfrac{\partial(\rho_s v_1)}{\partial y}+\dfrac{\partial(\rho_s w_1)}{\partial y}=0.\end{cases} \tag{14}$$

### 4.2 *Derivation of the KdV equation*

To address Eqs (13) and (14), we introduce

$$\begin{cases}\rho_s u_i=U_i,\\ \rho_s v_i=V_i,\\ \rho_s w_i=W_i,\\ \rho_s\theta_i=\Theta_i,\\ p_i=P_i,\end{cases} \tag{15}$$

where *i*=0, 1. Substituting Eq. (15) into Eqs (13) and (14) converts them into the following forms:

$$\begin{cases}(\bar{u}-c)\dfrac{\partial U_i}{\partial \xi}+(\bar{u}_y-y)V_i+(\bar{u}_z+\alpha)W_i+\dfrac{\partial P_i}{\partial \xi}=A_{u_i},\\ \dfrac{\partial P_i}{\partial y}+yU_i=A_{v_i},\\ \dfrac{\partial P_i}{\partial z}-\Theta_i=A_{w_i},\\ (\bar{u}-c)\dfrac{\partial \Theta_i}{\partial \xi}+\bar{\theta}_y V_i+W_i=A_{\theta_i},\\ \dfrac{\partial U_i}{\partial \xi}+\dfrac{\partial V_i}{\partial y}+\dfrac{\partial W_i}{\partial y}=0,\end{cases} \tag{16}$$

where

$$\begin{cases}A_{u_0}=0,\\ A_{v_0}=0,\\ A_{w_0}=\lambda\rho_s\bar{u},\\ A_{\theta_0}=0,\end{cases} \tag{17}$$

and

$$\begin{cases}A_{u_1}=-\left[\dfrac{\partial U_0}{\partial T}+\dfrac{1}{\rho_s}\left(U_0\dfrac{\partial U_0}{\partial \xi}+V_0\dfrac{\partial U_0}{\partial y}\right)+W_0\dfrac{\partial}{\partial z}\left(\dfrac{U_0}{\rho_s}\right)\right],\\ A_{v_1}=-(\bar{u}-c)\dfrac{\partial V_0}{\partial \xi},\\ A_{w_1}=\lambda U_0,\\ A_{\theta_1}=-\left[\dfrac{\partial \Theta_0}{\partial T}+\dfrac{1}{\rho_s}\left(U_0\dfrac{\partial \Theta_0}{\partial \xi}+V_0\dfrac{\partial \Theta_0}{\partial y}\right)\right].\end{cases} \tag{18}$$

According to Eq. (16), we have

$$(\bar{u}-c)\frac{\partial^2 P_i}{\partial z\partial \xi}+\bar{\theta}_y V_i+W_i=(\bar{u}-c)\frac{\partial A_{w_i}}{\partial \xi}+A_{\theta_i}, \tag{19}$$

and

$$\begin{aligned}&y(\bar{u}_y-y)V_i+y(\bar{u}_z+\alpha)W_i+y\frac{\partial P_i}{\partial \xi}-(\bar{u}-c)\frac{\partial^2 P_i}{\partial y\partial \xi}=\\ &yA_{u_i}-(\bar{u}-c)\frac{\partial A_{v_i}}{\partial \xi}.\end{aligned} \tag{20}$$

Moreover,

$$\begin{aligned}V_i=&\frac{1}{y[(\bar{u}_y-y)-\bar{\theta}_y(\bar{u}_z+\alpha)]}\times\\ &\left\{y(\bar{u}-c)(\bar{u}_z+\alpha)\frac{\partial^2 P_i}{\partial z\partial \xi}-y\frac{\partial P_i}{\partial \xi}+(\bar{u}-c)\frac{\partial^2 P_i}{\partial y\partial \xi}-\right.\\ &\left.y(\bar{u}_z+\alpha)\left[(\bar{u}-c)\frac{\partial A_{w_i}}{\partial \xi}+A_{\theta_i}\right]+yA_{u_i}-(\bar{u}-c)\frac{\partial A_{v_i}}{\partial \xi}\right\},\end{aligned} \tag{21}$$

$$\begin{aligned}W_i=&(\bar{u}-c)\frac{\partial A_{w_i}}{\partial \xi}+A_{\theta_i}-(\bar{u}-c)\frac{\partial^2 P_i}{\partial z\partial \xi}-\\ &\frac{\bar{\theta}_y}{y[(\bar{u}_y-y)-\bar{\theta}_y(\bar{u}_z+\alpha)]}\times\\ &\left\{y(\bar{u}-c)(\bar{u}_z+\alpha)\frac{\partial^2 P_i}{\partial z\partial \xi}-y\frac{\partial P_i}{\partial \xi}+(\bar{u}-c)\frac{\partial^2 P_i}{\partial y\partial \xi}-\right.\\ &\left.y(\bar{u}_z+\alpha)\left[(\bar{u}-c)\frac{\partial A_{w_i}}{\partial \xi}+A_{\theta_i}\right]+yA_{u_i}-(\bar{u}-c)\frac{\partial A_{v_i}}{\partial \xi}\right\}.\end{aligned} \tag{22}$$

The second equation of Eq. (16) becomes

$$\frac{\partial U_i}{\partial \xi}=\frac{1}{y}\left(\frac{\partial A_{v_i}}{\partial \xi}-\frac{\partial^2 P_i}{\partial y\partial \xi}\right). \tag{23}$$

Substitutions of Eqs (21)–(23) into the fifth equation of Eq. (16) lead to the PDEs with respect to $P_i$

$$L(P_i)=L_1\left(\frac{\partial A_{v_i}}{\partial \xi}\right)+L_2\left(\frac{\partial A_{w_i}}{\partial \xi}\right)+L_3(A_{\theta_i})+L_4(A_{u_i}), \tag{24}$$

where the operators are

$$L(\cdot)=-\frac{1}{y}\frac{\partial^2}{\partial y\partial\xi}(\cdot)+\frac{\partial}{\partial y}\left[\frac{(\bar{u}-c)(\bar{u}_z+\alpha)}{(\bar{u}_y-y)-\overline{\theta}_y(\bar{u}_z+\alpha)}\frac{\partial^2}{\partial z\partial\xi}(\cdot)\right]-\frac{\partial}{\partial y}\left[\frac{1}{(\bar{u}_y-y)-\overline{\theta}_y(\bar{u}_z+\alpha)}\frac{\partial}{\partial\xi}(\cdot)\right]+\frac{\partial}{\partial y}\left[\frac{(\bar{u}-c)(\bar{u}_z+\alpha)}{(\bar{u}_y-y)-\overline{\theta}_y(\bar{u}_z+\alpha)}\frac{\partial^2}{\partial y\partial\xi}(\cdot)\right]+\frac{\partial}{\partial z}\left[(\bar{u}-c)\frac{\partial^2}{\partial z\partial\xi}(\cdot)\right]-\frac{\partial}{\partial z}\left[\overline{\theta}_y\frac{(\bar{u}-c)(\bar{u}_z+\alpha)}{(\bar{u}_y-y)-\overline{\theta}_y(\bar{u}_z+\alpha)}\frac{\partial^2}{\partial z\partial\xi}(\cdot)\right]+\frac{\partial}{\partial z}\left[\overline{\theta}_y\frac{1}{(\bar{u}_y-y)-\overline{\theta}_y(\bar{u}_z+\alpha)}\frac{\partial}{\partial\xi}(\cdot)\right]+\frac{\partial}{\partial z}\left[\frac{\overline{\theta}_y(\bar{u}-c)}{y((\bar{u}_y-y)-\overline{\theta}_y(\bar{u}_z+\alpha))}\frac{\partial^2}{\partial\xi\partial y}(\cdot)\right],$$

$$L_1(\cdot)=-\frac{1}{y}(\cdot)+\left[\frac{(\bar{u}-c)}{y(\bar{u}_y-y-\overline{\theta}_y(\bar{u}_z+\alpha))}\right]_y(\cdot)+\frac{\partial}{\partial z}\left[\frac{\overline{\theta}_y(\bar{u}-c)}{y((\bar{u}_y-y)-\overline{\theta}_y(\bar{u}_z+\alpha))}(\cdot)\right],$$

$$L_2(\cdot)=\frac{\partial}{\partial y}\left[\frac{(\bar{u}-c)(\bar{u}_z+\alpha)}{(\bar{u}_y-y)-\overline{\theta}_y(\bar{u}_z+\alpha)}(\cdot)\right]-\frac{\partial}{\partial z}\left[(\bar{u}-c)(\cdot)\right]+\frac{\partial}{\partial z}\left[\frac{(\bar{u}-c)(\bar{u}_z+\alpha)\overline{\theta}_y}{(\bar{u}_y-y)-\overline{\theta}_y(\bar{u}_z+\alpha)}(\cdot)\right],$$

$$L_3(\cdot)=\frac{\partial}{\partial y}\left[\frac{(\bar{u}_z+\alpha)}{(\bar{u}_y-y)-\overline{\theta}_y(\bar{u}_z+\alpha)}(\cdot)\right]+\frac{\partial}{\partial z}\left[\frac{(\bar{u}_z+\alpha)\overline{\theta}_y}{(\bar{u}_y-y)-\overline{\theta}_y(\bar{u}_z+\alpha)}(\cdot)\right],$$

$$L_4(\cdot)=-\frac{\partial}{\partial y}\left[\frac{1}{(\bar{u}_y-y)-\overline{\theta}_y(\bar{u}_z+\alpha)}(\cdot)\right]-\frac{\partial}{\partial z}\left[\frac{\overline{\theta}_y}{(\bar{u}_y-y)-\overline{\theta}_y(\bar{u}_z+\alpha)}(\cdot)\right].$$

For $i=0$, it is easy to obtain

$$L(P_0)=0. \tag{25}$$

Thus, we obtain the solutions:

$$\begin{cases}P_0=\tilde{p}_0(y,z)n(T,\xi),\\ U_0=\tilde{u}_0(y,z)n(T,\xi),\\ V_0=\tilde{v}_0(y,z)\dfrac{\partial n(T,\xi)}{\partial\xi},\\ W_0=\tilde{w}_0(y,z)\dfrac{\partial n(T,\xi)}{\partial\xi},\\ \Theta_0=\tilde{\theta}_0(y,z)n(T,\xi),\end{cases} \tag{26}$$

Further,

$$\begin{cases}A_{u_1}=-\left[\dfrac{\partial n_0}{\partial T}\tilde{u}_0+\dfrac{1}{\rho_s}n_0\dfrac{\partial n_0}{\partial\xi}\left(\tilde{u}_0^2+\tilde{v}_0\dfrac{\partial\tilde{u}_0}{\partial y}+\tilde{w}_0\dfrac{\partial\tilde{u}_0}{\partial z}\right)\right],\\ A_{v_1}=-(\bar{u}-c)\dfrac{\partial^2 n_0}{\partial\xi^2}\tilde{v}_0,\\ A_{w_1}=\lambda n_0\tilde{u}_0,\\ A_{\theta_1}=-\left[\dfrac{\partial n_0}{\partial T}\tilde{\theta}_0+\dfrac{1}{\rho_s}n_0\dfrac{\partial n_0}{\partial\xi}\left(\tilde{u}_0\tilde{\theta}_0+\tilde{v}_0\dfrac{\partial\tilde{\theta}_0}{\partial y}\right)\right].\end{cases} \tag{27}$$

Thus, Eq. (25) is simplified as

$$L_{y,z}(\tilde{p}_0)=0, \tag{28}$$

where

$$L_{y,z}(\cdot)=-\frac{1}{y}\frac{\partial}{\partial y}(\cdot)+\frac{\partial}{\partial y}\left[\frac{(\bar{u}-c)(\bar{u}_z+\alpha)}{(\bar{u}_y-y)-\overline{\theta}_y(\bar{u}_z+\alpha)}\frac{\partial}{\partial z}(\cdot)\right]-\frac{\partial}{\partial y}\left[\frac{1}{(\bar{u}_y-y)-\overline{\theta}_y(\bar{u}_z+\alpha)}(\cdot)\right]+\frac{\partial}{\partial y}\left[\frac{(\bar{u}-c)(\bar{u}_z+\alpha)}{(\bar{u}_y-y)-\overline{\theta}_y(\bar{u}_z+\alpha)}\frac{\partial}{\partial y}(\cdot)\right]+\frac{\partial}{\partial z}\left[(\bar{u}-c)\frac{\partial}{\partial z}(\cdot)\right]-\frac{\partial}{\partial z}\left[\overline{\theta}_y\frac{(\bar{u}-c)(\bar{u}_z+\alpha)}{(\bar{u}_y-y)-\overline{\theta}_y(\bar{u}_z+\alpha)}\frac{\partial}{\partial z}(\cdot)\right]+\frac{\partial}{\partial z}\left[\overline{\theta}_y\frac{1}{(\bar{u}_y-y)-\overline{\theta}_y(\bar{u}_z+\alpha)}(\cdot)\right]+\frac{\partial}{\partial z}\left[\frac{\overline{\theta}_y(\bar{u}-c)}{y((\bar{u}_y-y)-\overline{\theta}_y(\bar{u}_z+\alpha))}\frac{\partial}{\partial y}(\cdot)\right]. \tag{29}$$

Equation (24) has the same homogeneous term for the cases $i$=0 and $i$=1. To satisfy the nonsingularity of the solution, the following is required:

$$\iint_{y,z}\frac{\tilde{p}_0^*}{\bar{u}-c}\left(L_1\left(\frac{\partial A_{v_1}}{\partial\xi}\right)+L_2\left(\frac{\partial A_{w_1}}{\partial\xi}\right)+L_3(A_{\theta_1})+L_4(A_{u_1})\right)\mathrm{d}y\mathrm{d}z=0, \tag{30}$$

where $\tilde{p}_0^*$ is the solution for the conjugate equation of Eq. (28). Then, Eq. (30) becomes the following form:

$$I\frac{\partial n_0}{\partial T}+I_1\frac{\partial n_0}{\partial\xi}+I_2 n_0\frac{\partial n_0}{\partial\xi}+I_3\frac{\partial^3 n_0}{\partial\xi^3}=0, \tag{31}$$

where the coefficients $I,\ I_1,\ I_2,\ I_3$ are

$$I=-\iint_{y,z}\frac{\tilde{p}_0^*}{\bar{u}-c}\left(L_3(\tilde{\theta}_0)+L_4(\tilde{u}_0)\right)\mathrm{d}y\mathrm{d}z,$$

$$I_1=\lambda\iint_{y,z}\frac{\tilde{p}_0^*}{\bar{u}-c}L_2(\tilde{u}_0)\mathrm{d}y\mathrm{d}z,$$

$$I_2 = -\iint\limits_{y,z} \frac{\tilde{p}_0^*}{\bar{u}-c}\left\{L_3\left[\frac{1}{\rho_s}\left(\tilde{u}_0\tilde{\theta}_0+\tilde{v}_0\frac{\partial\tilde{\theta}_0}{\partial y}\right)\right]+ L_4\left[\frac{1}{\rho_s}\left(\tilde{u}_0^2+\tilde{v}_0\frac{\partial\tilde{u}_0}{\partial y}+\tilde{w}_0\frac{\partial\tilde{u}_0}{\partial z}\right)\right]\right\}\mathrm{d}y\mathrm{d}z,$$

$$I_3 = -\iint\limits_{y,z} \frac{\tilde{p}_0^*}{\bar{u}-c}L_1[(\bar{u}-c)\tilde{v}_0]\mathrm{d}y\mathrm{d}z.$$

Eqation (31) is the well-known KdV equation. Special attention is paid to the coefficient $I_1$, which shows that the horizontal component of Coriolis parameters is also an important factor affecting near-inertial waves in the equatorial atmosphere by modifying the velocity characteristic of the waves. This is consistent with the result of Rossby waves accompanying topography under the complete Coriolis force by Yang et al. (2016). However, the topography is not a necessary factor in our present study. On the other hand, the effect of $\alpha$ on the wave is mainly reflected in a combined way with the vertical shear of the basic flow, i.e., $\bar{u}_z$, it is a result that cannot be obtained under the traditional approximation. When the horizontal component of the Coriolis parameters is not considered, the equations become the shallow water model, and then Eq. (31) is reduced to the traditional case.

### 4.3 *The periodic and solitary solutions of the KdV equation*

Equation (31) is simplified into

$$\frac{\partial A}{\partial T}+a_1 A\frac{\partial A}{\partial \xi}+a_2\frac{\partial^3 A}{\partial \xi^3}+a_3\frac{\partial A}{\partial \xi}=0, \tag{32}$$

where $a_1=\frac{I_2}{I}, a_2=\frac{I_3}{I}, a_3=\frac{I_1}{I}$.

Many kinds of exact analytical methods have been proposed in recent years to solve nonlinear evolution equations, such as solitary waves. In what follows, we mainly adopt the method of Jacobian elliptic function expansions to solve Eq. (32). Introduce an appropriate ansatz $X=k(\xi-c_1T)$, where $k$ is the wavenumber and $c_1$ is the wave velocity. Thus, Eq. (32) is

$$(a_3-c_1)\frac{\mathrm{d}A}{\mathrm{d}X}+a_1 A\frac{\mathrm{d}A}{\mathrm{d}X}+a_2k^2\frac{\mathrm{d}^3A}{\mathrm{d}X^3}=0. \tag{33}$$

According to the method of Jacobian elliptic function expansions, $A(X)$ has the formal solution as a finite summation of $sn\,X$:

$$A(X)=\sum_{j=0}^{n} b_j sn^j X, \tag{34}$$

where $n=2$ is a necessary condition for the balance between the nonlinearity and dispersion; then, we obtain

$$A(X)=b_0+b_1 sn\,X+b_2 sn^2 X. \tag{35}$$

By using the properties of elliptic functions, the solution is

$$A(\xi,T)=\frac{4a_2k^2(1+m^2)+c_1-a_3}{a_1}-\frac{12a_2k^2m^2}{a_1}sn^2k(\xi-c_1T). \tag{36}$$

When $m\to 1$, the solitary wave solution is

$$A(\xi,T)=\frac{c_1-a_3-4a_2k^2}{a_1}+\frac{12a_2k^2}{a_1}\mathrm{sech}^2k(\xi-c_1T), \tag{37}$$

especially, when $c_1–a_3-4a_2k^2=0$, the solitary solution becomes

$$A(\xi,T)=\frac{3(c_1-a_3)}{a_1}\mathrm{sech}^2\sqrt{\frac{c_1-a_3}{4a_2}}(\xi-c_1T). \tag{38}$$

Obviously, both the periodic and solitary wave solutions show that the effect of the Coriolis horizontal component on the equatorial nonlinear wave is mainly reflected by modifying the wave velocity but not the wave amplitude or wave energy.

## 5 Results

In this section, we devote ourselves to the dynamic analysis of the effect of the horizontal Coriolis parameter on the nonlinear equatorial near-inertial solitary waves through numerical simulations. According to the previous scale analysis, the effect of parameter $\alpha$ is much smaller than $\lambda$. Thus, in what follows, we mainly discuss the dynamic effect of the horizontal component of Coriolis parameters through $\lambda$, which means that the coefficient of $a_3$ represents the main function of the Coriolis horizontal component on the evolution of equatorial near-inertial solitary waves. In addition, it is acceptable to perform some coordinate transformations so that all the coefficients of Eq. (32) become one, with the popular Fourier spectral method for Eq. (32) with fixed $a_1=a_2=1$ and varied $a_3$. An initial solitary wave solution is assumed to be $\mathrm{sech}^2\xi$.

Figure 1 depicts the whole evolution processes of the solitary equatorial near-inertial waves under the nontraditional approximation. From the figure, we can see that the initial solitary wave $\mathrm{sech}^2\xi$ evolves to the west and east along with time, the magnitude of the amplitude decreases with time in both directions, and the solitary wave packets are excited when the solitary waves are propagating. On the other hand, it is interesting to find that the asymmetry structures of the wave packets with respect to zonal spatial coordinates are formulated during its evolutionary process. It denotes that the solitary wave is propagating to the west with higher speed and frequencies, it is consistent with some existed results, such as the work (Gerkema and Shrira, 2005a, 2005b). In order to disclose the effect of the horizontal component of the Coriolis parameters more clearly, two-dimensional projections of the propagation process are given in Fig. 2.

In Fig. 2, the evolution of the solitary wave amplitude in the

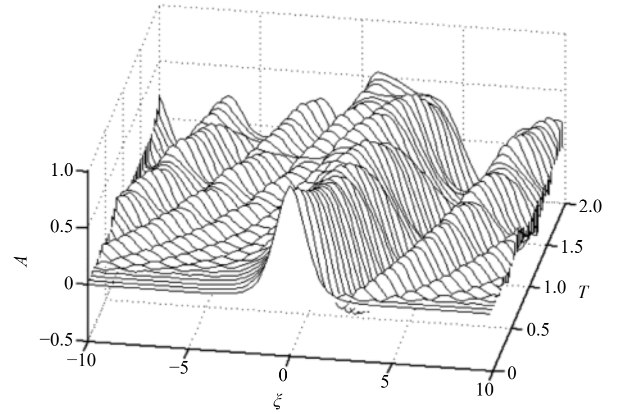


**Fig. 1.** The evolution processes of wave magnitude with time and space.

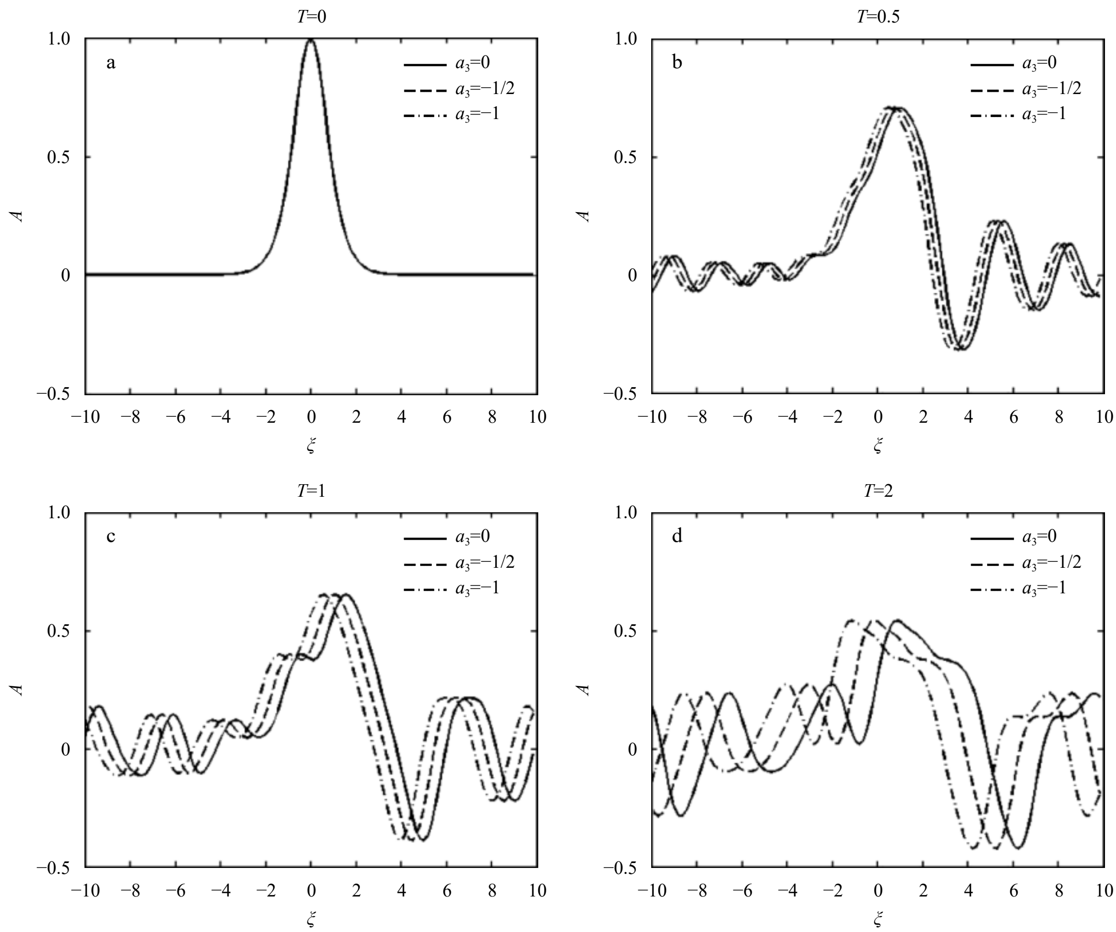


**Fig. 2.** The dynamic effect of the horizontal Coriolis parameter on the evolution of solitary wave.

two-dimensional case with different $a_3$ is characterized, which means that the horizontal Coriolis parameter varies affects the evolution of solitary waves. We can find that the initial solitary wave evolves into wave packets to both west and east with time goes. It is obvious that $a_3$ affects the wave velocity. It denotes that larger magnitude of $a_3$ increases the westward propagation of solitary waves. Furthermore, it is to say that the dispersion relationship is essentially modified by the consideration of complete Coriolis parameters, it is consistent with the former qualitative analysis for Eq. (31).

## 6 Conclusions

Traditional investigations on inertial waves neglect the effect of complete Coriolis parameters, leading to qualitative inaccuracy. This paper is the first to investigate the effect of the horizontal Coriolis parameter on nonlinear equatorial near-inertial waves. Detailed scale analysis is given based on the primitive mesoscale oceanic model equations, and it denotes that a necessary condition for the inclusion of the complete Coriolis parameter is the three-dimensional oceanic motion. The evolution of the equatorial near-inertial wave was proven to be satisfied with the classical KdV model equation, and the coefficients related to the horizontal Coriolis parameter were denoted to affect the evolution of solitary waves by mainly modifying the wave speed and by interacting with the basic flow. The Fourier spectral method was used to verify the dynamic mechanisms.

In recent years, more and more investigations were finished to disclose the potential influences of complete Coriolis parameters on kinds of oceanic motions. Tort et al. (2016) and Kloosterziel et al. (2017) studied the inertial asymmetry and instability problem with complete Coriolis force by numerical simulations, the results of the present paper are consistent with those in their papers. Thus, the theoretical analysis results of this paper may be potentially contributed to the understanding of oceanic near-inertial waves. More importantly, much more attentions should be further paid to the observational or experimental results to verify the consistency of the present theoretical analysis in our further investigations.

## References

Benney D J. 1966. Long non-linear waves in fluid flows. Journal of Mathematics and Physics, 45(1–4): 52–63

Caillol P, Grimshaw R H. 2008. Rossby elevation waves in the presence of a critical layer. Studies in Applied Mathematics, 120(1): 35–64

Caldwell D R. 1983. Small-scale physics of the ocean. Reviews of Geophysics, 21(5): 1192–1205

Fruman M D. 2009. Equatorially bounded zonally propagating linear waves on a generalized $\beta$ plane. Journal of the Atmospheric Sciences, 66(9): 2937–2945

Fu Lei, Chen Yaodeng, Yang Hongwei. 2019. Time-space fractional coupled generalized Zakharov-Kuznetsov equations set for Rossby solitary waves in two-layer fluids. Mathematics, 7(1): 41

Fu Lei, Yang Hongwei. 2019. An application of (3+1)-dimensional time-space fractional ZK model to analyze the complex dust acoustic waves. Complexity, 2019: 2806724

Gerkema T, Shrira V I. 2005a. Near-inertial waves on the “nontraditional” $\beta$ plane. Journal of Geophysical Research: Oceans,

110(C1): C01003
Gerkema T, Shrira V I. 2005b. Near-inertial waves in the ocean: Beyond the "traditional approximation". Journal of Fluid Mechanics, 529: 195–219
Gerkema T, Zimmerman J T F, Maas L R M, et al. 2008. Geophysical and astrophysical fluid dynamics beyond the traditional approximation. Reviews of Geophysics, 46(2): RG2004
Grimshaw R H J. 1975. A note on the $\beta$-plane approximation. Tellus, 27(4): 351–357
Guo Min, Dong Haoyu, Liu Jianxin, et al. 2019. The time-fractional mZK equation for gravity solitary waves and solutions using sech-tanh and radial basic function method. Nonlinear Analysis: Modelling and Control, 24(1): 1–19
Hayashi M, Itoh H. 2012. The importance of the nontraditional Coriolis terms in large-scale motions in the tropics forced by prescribed cumulus heating. Journal of the Atmospheric Sciences, 69(9): 2699–2716
Helal M A, Seadawy A R. 2012. Benjamin-Feir instability in nonlinear dispersive waves. Computers & Mathematics with Applications, 64(11): 3557–3568
Holton J R, Hakim G J. 2013. An Introduction to Dynamic Meteorology. 5th ed. Boston: Academic Press
Itano T, Kasahara A. 2011. Effect of top and bottom boundary conditions on symmetric instability under full-component Coriolis force. Journal of the Atmospheric Sciences, 68(11): 2771–2782
Kasahara A. 2003. On the nonhydrostatic atmospheric models with inclusion of the horizontal component of the earth's angular velocity. Journal of the Meteorological Society of Japan. Ser. Ⅱ, 81(5): 935–950
Kasahara A. 2010. A mechanism of deep-ocean mixing due to near-inertial waves generated by flow over bottom topography. Dynamics of Atmospheres and Oceans, 49(2–3): 124–140
Khater A H, Callebaut D K, Helal M A, et al. 2006a. Variational method for the nonlinear dynamics of an elliptic magnetic stagnation line. The European Physical Journal D-Atomic, Molecular, Optical and Plasma Physics, 39(2): 237–245
Khater A H, Callebaut D K, Seadawy A R. 2006b. General soliton solutions for nonlinear dispersive waves in convective type instabilities. Physica Scripta, 74(3): 384–393
Kloosterziel R C, Carnevale G F, Orlandi P. 2007. Inertial instability in rotating and stratified fluids: barotropic vortices. Journal of Fluid Mechanics, 583: 379–412
Kloosterziel R C, Carnevale G F, Orlandi P. 2017. Equatorial inertial instability with full Coriolis force. Journal of Fluid Mechanics, 825: 69–108
Leibovich S, Lele S K. 1985. The influence of the horizontal component of earth's angular velocity on the instability of the Ekman layer. Journal of Fluid Mechanics, 150: 41–87
Liu Yongjun, Gao Xiaoping, Yu Tianxia, et al. 2015. Influence of complete Coriolis force on the dispersion relation of ocean internal-wave in a background currents field. MATEC Web of Conferences, 25: 01014
Long R R. 1964. Solitary waves in the westerlies. Journal of the Atmospheric Sciences, 21(2): 197–200
Marshall J, Schott F. 1999. Open-ocean convection: Observations, theory, and models. Reviews of Geophysics, 37(1): 1–64
Nezlin M V, Snezhkin E N. 1993. Rossby Vortices, Spiral Structures, Solitons. Berlin: Springer-Verlag
Ono H. 1981. Algebraic Rossby wave soliton. Journal of the Physical Society of Japan, 50(8): 2757–2761
Pedlosky J. 1987. Geophysical Fluid Dynamics. New York: Springer-Verlag
Phillips N A. 1966. The equations of motion for a shallow rotating atmosphere and the "traditional approximation". Journal of the Atmospheric Sciences, 23(5): 626–628
Ren Yanwei, Tao Mengshuang, Dong Huanhe, et al. 2019. Analytical research of (3+1)-dimensional Rossby waves with dissipation effect in cylindrical coordinate based on Lie symmetry approach. Advances in Difference Equations, 2019: 13
Satsuma J, Ablowitz M J, Kodama Y. 1979. On an internal wave equation describing a stratified fluid with finite depth. Physics Letters A, 73(4): 283–286
Seadawy A R. 2011. New exact solutions for the KdV equation with higher order nonlinearity by using the variational method. Computers & Mathematics with Applications, 62(10): 3741–3755
Seadawy A R. 2015. Nonlinear wave solutions of the three-dimensional Zakharov-Kuznetsov-Burgers equation in dusty plasma. Physica A: Statistical Mechanics and its Applications, 439: 124–131
Seadawy A R. 2016. Stability analysis solutions for nonlinear three-dimensional modified Korteweg-de Vries-Zakharov-Kuznetsov equation in a magnetized electron-positron plasma. Physica A: Statistical Mechanics and its Applications, 455: 44–51
Seadawy A R. 2017a. Two-dimensional interaction of a shear flow with a free surface in a stratified fluid and its solitary-wave solutions via mathematical methods. The European Physical Journal Plus, 132(12): 518
Seadawy A R. 2017b. Solitary wave solutions of two-dimensional nonlinear Kadomtsev-Petviashvili dynamic equation in dust-acoustic plasmas. Pramana, 89(3): 49
Seadawy A R. 2018. Three-dimensional weakly nonlinear shallow water waves regime and its traveling wave solutions. International Journal of Computational Methods, 15(3): 1850017
Seadawy A R, Alamri S Z. 2018. Mathematical methods via the nonlinear two-dimensional water waves of Olver dynamical equation and its exact solitary wave solutions. Results in Physics, 8: 286–291
Seadawy A R, Lu D C, Yue C. 2017. Travelling wave solutions of the generalized nonlinear fifth-order KdV water wave equations and its stability. Journal of Taibah University for Science, 11(4): 623–633
Tian Runhua, Fu Lei, Ren Yanwei, et al. 2019. (3+1)-Dimensional time-fractional modified Burgers equation for dust ion-acoustic waves as well as its exact and numerical solutions. Mathematical Methods in the Applied Science, 1–20
Tort M, Ribstein B, Zeitlin V. 2016. Symmetric and asymmetric inertial instability of zonal jets on the f-plane with complete Coriolis force. Journal of Fluid Mechanics, 788: 274–302
White A A, Bromley R A. 1995. Dynamically consistent, quasi-hydrostatic equations for global models with a complete representation of the Coriolis force. Quarterly Journal of the Royal Meteorological Society, 121(522): 399–418
Yang Hongli, Liu Fumei, Wang Danni, et al. 2016. Nonlinear Rossby waves near the equator with complete Coriolis force. Progress in Geophysics (in Chinese), 31(3): 988–991
Yang Hongwei, Sun Junchao, Fu Chen. 2019. Time-fractional Benjamin-Ono equation for algebraic gravity solitary waves in baroclinic atmosphere and exact multi-soliton solution as well as interaction. Communications in Nonlinear Science and Numerical Simulation, 71: 187–201
Yano J I. 2017. Inertio-gravity waves under the non-traditional $f$-plane approximation: Singularity in the large-scale limit. Journal of Fluid Mechanics, 810: 475–488
Yasuda Y, Sato K. 2013. The effect of the horizontal component of the angular velocity of the earth's rotation on inertia-gravity waves. Journal of the Meteorological Society of Japan. Ser Ⅱ, 91(1): 23–41
Zhang Xiaoming. 1991. A model of the equatorial deep jets and the role of the horizontal Coriolis parameter [dissertation]. Woods Hole: Woods Hole Oceanographic Institution
Zhang Ruigang, Liu Quansheng, Yang Liangui, et al. 2019a. Nonlinear planetary-synoptic wave interaction under generalized beta effect and its solutions. Chaos, Solitons & Fractals, 122: 270–280
Zhang Ruigang, Yang Liangui. 2019. Nonlinear Rossby waves in zonally varying flow under generalized beta approximation. Dynamics of Atmospheres and Oceans, 85: 16–27
Zhang Ruigang, Yang Liangui, Liu Quansheng, et al. 2019b. Dynamics of nonlinear Rossby waves in zonally varying flow with spatial-temporal varying topography. Applied Mathematics and Computation, 346: 666–679